

Supplementary Information

Controlled Release of Chemically Diverse Small Molecules from Liquid-Core Capsules Assembled in Fully Aqueous Conditions

Rita C. Neves¹⁺, Bárbara S. Neves¹⁺, Bruno P. Morais¹, Raquel C. Gonçalves¹, João F. Mano¹, Mariana B. Oliveira^{1*}

¹ CICECO – Aveiro Institute of Materials, Department of Chemistry, University of Aveiro.
Campus Universitário de Santiago. 3810-193 Aveiro, Portugal

*equal author contribution

*Corresponding author. Email: Mariana B. Oliveira: mboliveira@ua.pt

Table S1. Comparison between waste generation of all-aqueous LbL capsule fabrication approach and the herein reported technology.

Route	Water waste (kg/batch)	Polymer solids waste (g/batch)	E-factor (incl. water)
Proposed technology	0.195	0.3375	0.195
LbL (10 bilayers)	1.045	0.2700	1.045

We compared the amount of used and discarded solvents of polymers, additives and water (solvent) in a typical sacrificial template-based LbL capsules manufacturing system, with the same amounts to produce the same number of capsules using the currently proposed technology. We based our calculations for LbL technology in reference ²³.

Ratio (LbL/ Current work): LbL uses ≈ 5.36 -fold more water per batch compared to the stated workflow. LbL polymers waste is ≈ 0.8 -fold lower.

The E-factor was calculated following eq. (1):

$$E - factor = \frac{\text{total mass of waste (kg)}}{\text{mass of product (kg)}} \quad (1)$$

Although the E-factor is not the same as water waste, in practice, since both processes are completely based on the use of water as a solvent, and the mass of the used polymers and additives is very small in comparison to the mass of water, the E-factors obtained for both technologies reflect a similar value to the water waste calculation presented in Table S1.

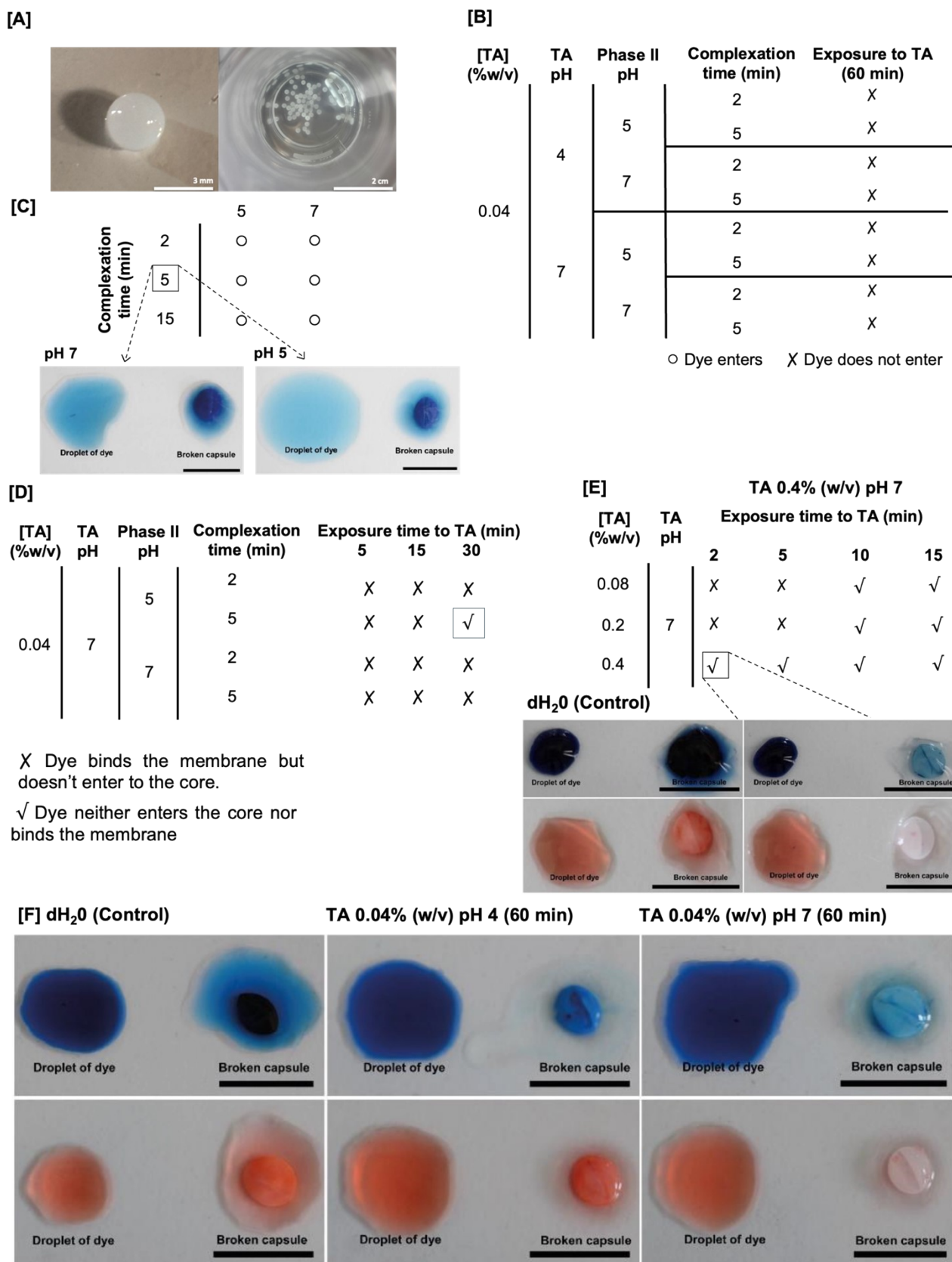


Fig. S1. Qualitative/observational results for optimizations of AR and MB entrance to capsules and interactions with the membranes. **[A]** Images of capsules after processing. **[B]** Analysis of the permeability of the capsules to dyes varying the complexation time and phase II pH value.

Encapsulation of methylene blue (MB, Mw=320 Da, positively charged). The complexation conditions to produce the capsules include a complexation time of 5 minutes and phase II pH value of 7. Encapsulation of methylene blue (MB, Mw=320 Da, positively charged). The complexation conditions to produce the capsules include a complexation time of 5 minutes and phase II pH value of 5. In the left side of each photo, there is a droplet of the medium at which the capsules were incubated with the dye; in the right side, there is a broken capsule and its dye release, highlighting the effects of a different pH on dye-membrane interaction. Scale bar: 1 cm. [C] Analysis of the permeability of the capsules to dyes after exposure to 0.04% TA, at either pH 4 or pH 7, for 60 minutes, varying the complexation time and phase II pH value. This table also indicates whether the dye enters the capsule core or binds only to the membrane. [D] Table summarizing further experimental conditions, showing the results for the analysis of the permeability of the capsules to dyes after exposure to 0.04% TA, at pH 7, for 5, 15 and 30 minutes, varying the complexation time and phase II pH value. [E] Experimental results for the analysis of the permeability of the capsules to dyes after exposure to TA solutions with different concentrations, for 2, 5, 10 and 15 minutes. The table shows when the dye enters the core or only binds to the membrane. Encapsulation of MB (Mw=320 Da, positively charged) (top) and AR (Mw=496 Da, negatively charged) (bottom). The complexation conditions to produce the capsules include phase II pH value of 5 and a complexation time of 5 minutes. The control capsules were soaked in dH₂O instead of TA, for 2 minutes. Control experiment shows the dye behavior in the absence of any TA treatment for comparison. Capsules were then soaked in 0.4% TA pH 7 for 2 minutes, washed with PBS, and dipped in the respective dye, highlighting the results of using a higher concentration of TA on the dye's behavior and capsule interaction. In the left of each figure, there is a droplet of the medium at which the capsules were incubated with the dye; in the right, there is a broken capsule and its content release. Scale bar: 1 cm. [F] Encapsulation of MB (Mw=320 Da, positively charged) (top) and AR (Mw=496 Da, negatively charged) (bottom). The complexation conditions to produce the capsules include phase II pH value of 5 and a complexation time of 5 minutes. Control capsules were soaked in dH₂O instead of TA, for 60 minutes. The figure shows the interaction of both dyes with the capsule in the absence of TA-treatment. Capsules were then soaked in 0.04% TA at pH 4 and 0.04% TA at pH 7 for 60 minutes, and dipped in the respective dye, showing the effect of this treatment on dye entrance and membrane binding. In left side of each figure, there is a droplet of the medium at which the capsules were incubated with the dye; in the right side, there is a broken capsule and its content release. Scale bar: 1 cm.

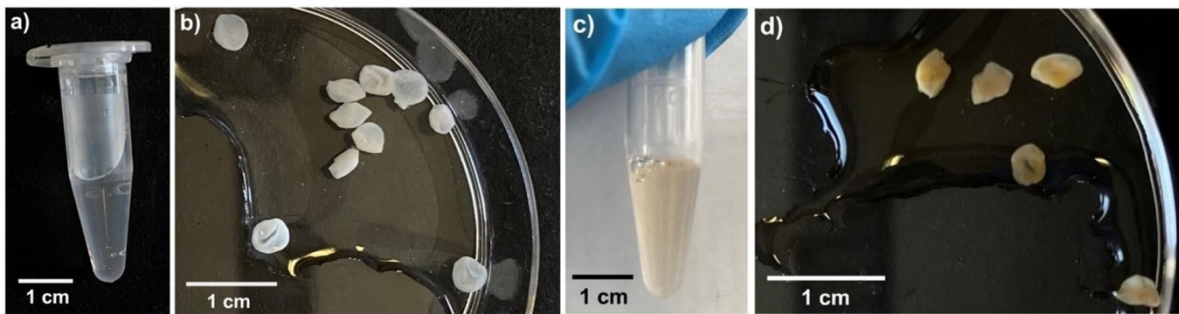


Fig. S2. Oxidation of the capsules with 10 M NaOH. **[A]** Inner content of control capsules after exposure to NaOH. **[B]** Membrane of control capsules after exposure to NaOH. **[C]** Inner content of TA-treated capsules after exposure to NaOH. **[D]** Membrane of TA-treated capsules after exposure to NaOH.

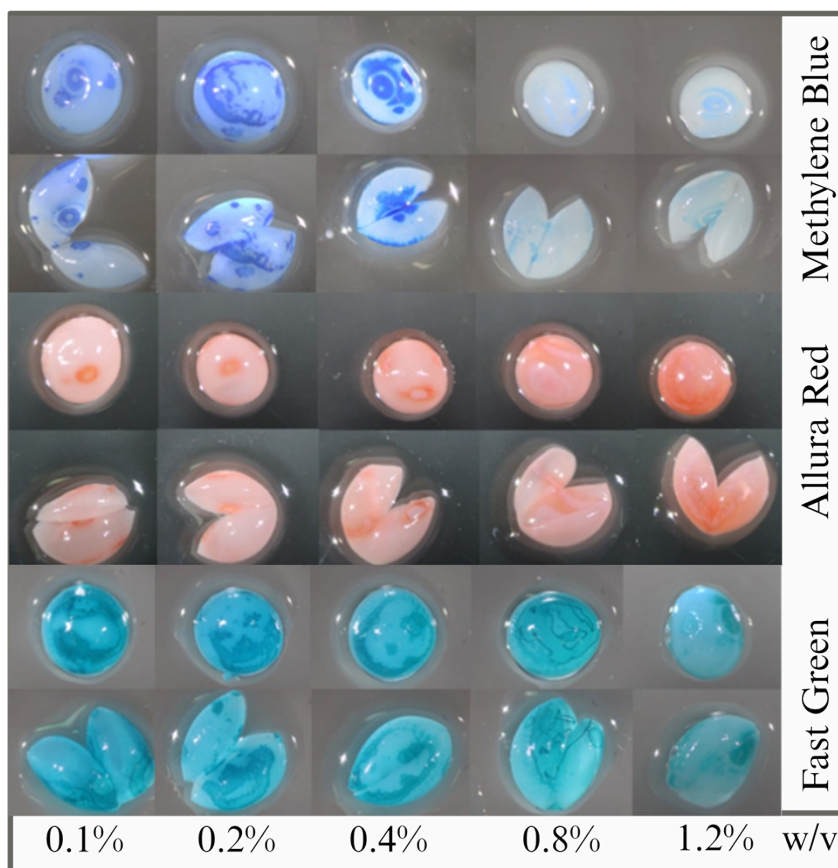


Fig. S3. Representative images of capsules treated with different concentrations of TA in contact with AR, MB and FG. The membrane was inspected after 1 hour immersion in dye solutions, as well as the inner liquid, in which the presence of dyes was assessed

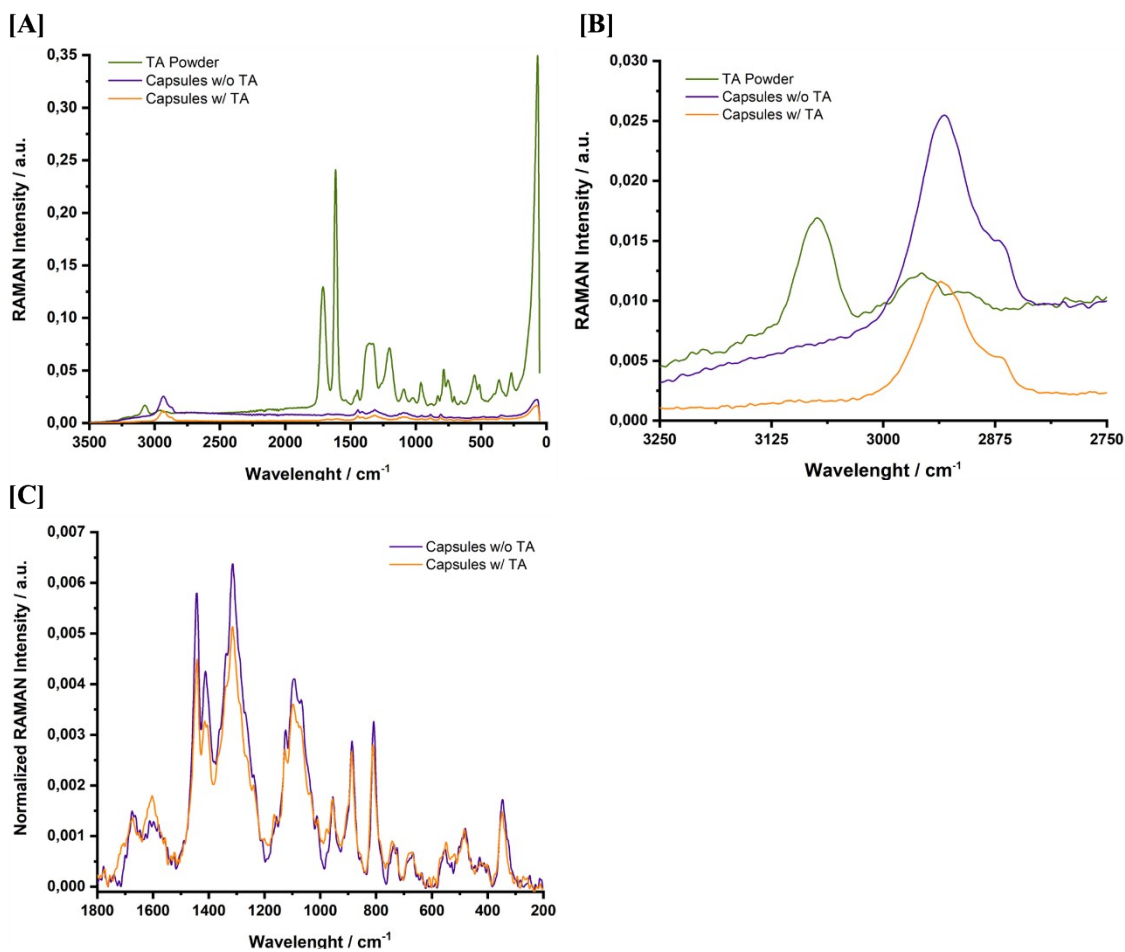


Fig. S4. **[A]** Raman spectra ($\lambda_{exc} = 1064$ nm) of polyelectrolyte liquid-core capsules and tannic acid powder. Capsules were freeze-dried prior to analysis. **[B]** Expanded Raman spectra in the 3250-2750 cm^{-1} region of tannic acid powder, alginate/e-poly-L-lysine control capsules and TA-treated capsules. **[C]** Expanded normalized spectra, in the 1800-200 cm^{-1} region of capsule systems and tannic acid powder, highlighting aromatic vibrational modes of TA. In all graphs, brown lines denote tannic acid powder; purple lines indicate control capsules; and solid orange lines represent TA-treated capsules.

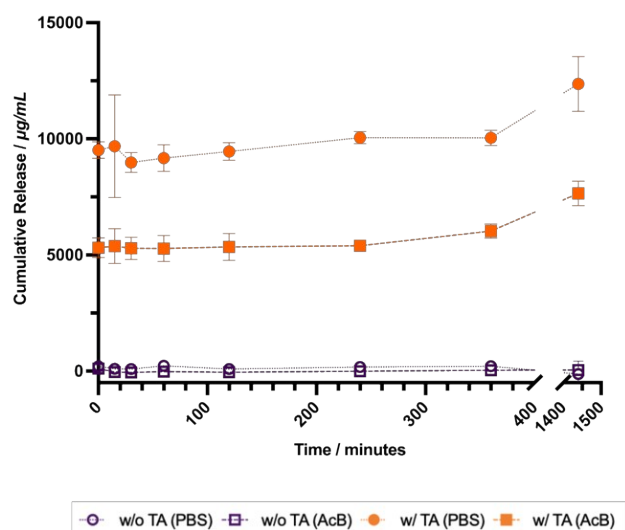


Fig. S5. Cumulative release of TA from capsules immersed in different buffers at pH 4 or 7.4.

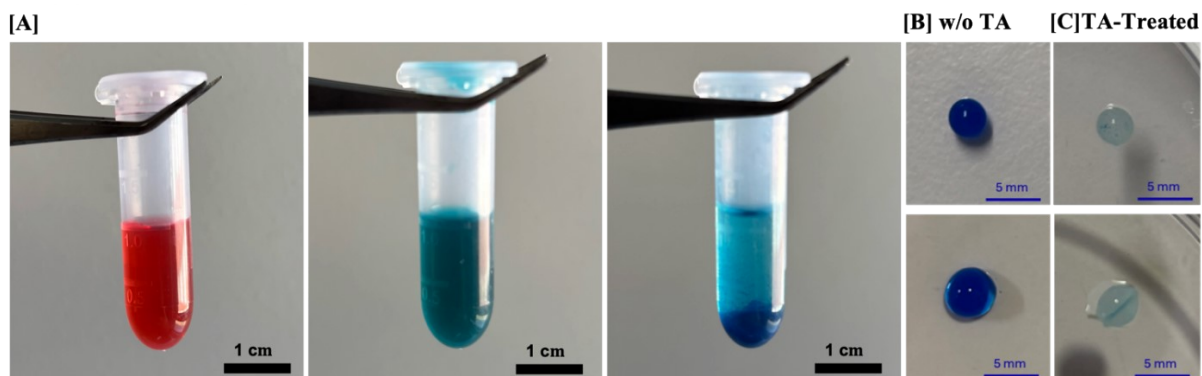


Fig. S6. [A] Interaction of 0.4% TA mixed directly with Allura red (left), Fast Green (middle) and Methylene Blue (right) at pH 7.4. Visual representation of permeability and dye-membrane interactions, after 1 hour of MB incubation, in capsules non-treated [B] and TA-treated [C].

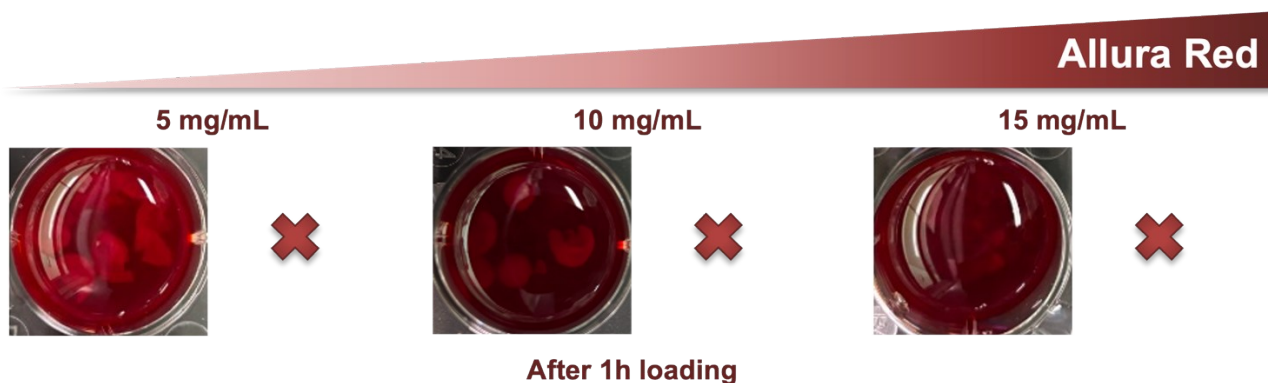


Fig. S7. Pictures of non-treated capsules during AR loading. It is visible at for concentrations higher than 2.5 mg/mL, capsule structure is compromised, probably due to the competition of AR negative charges with the polyelectrolyte-polyelectrolyte interactions in the capsule membranes.

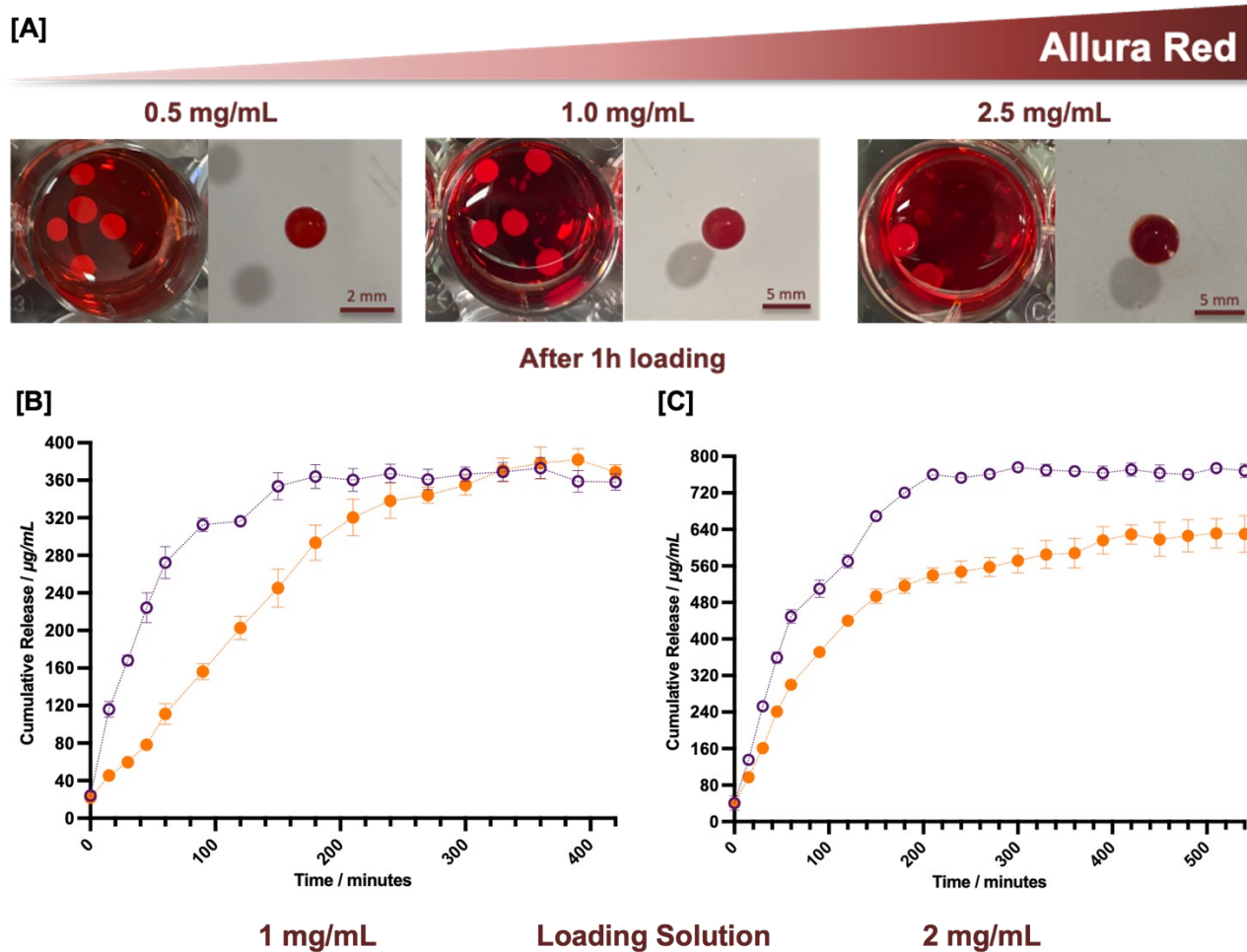


Fig. S8. [A] Pictures of non-treated capsules during AR loading. Different concentrations of AR have been tested to achieve the limit of small molecule that could be encapsulated, without cause damage to the polyelectrolyte capsule, namely 0.5 mg/mL; 1.0 mg/mL and 2.5 mg/mL [B] Release of AR in PBS for 1 mg/mL; and [C] 2 mg/mL loading concentrations.

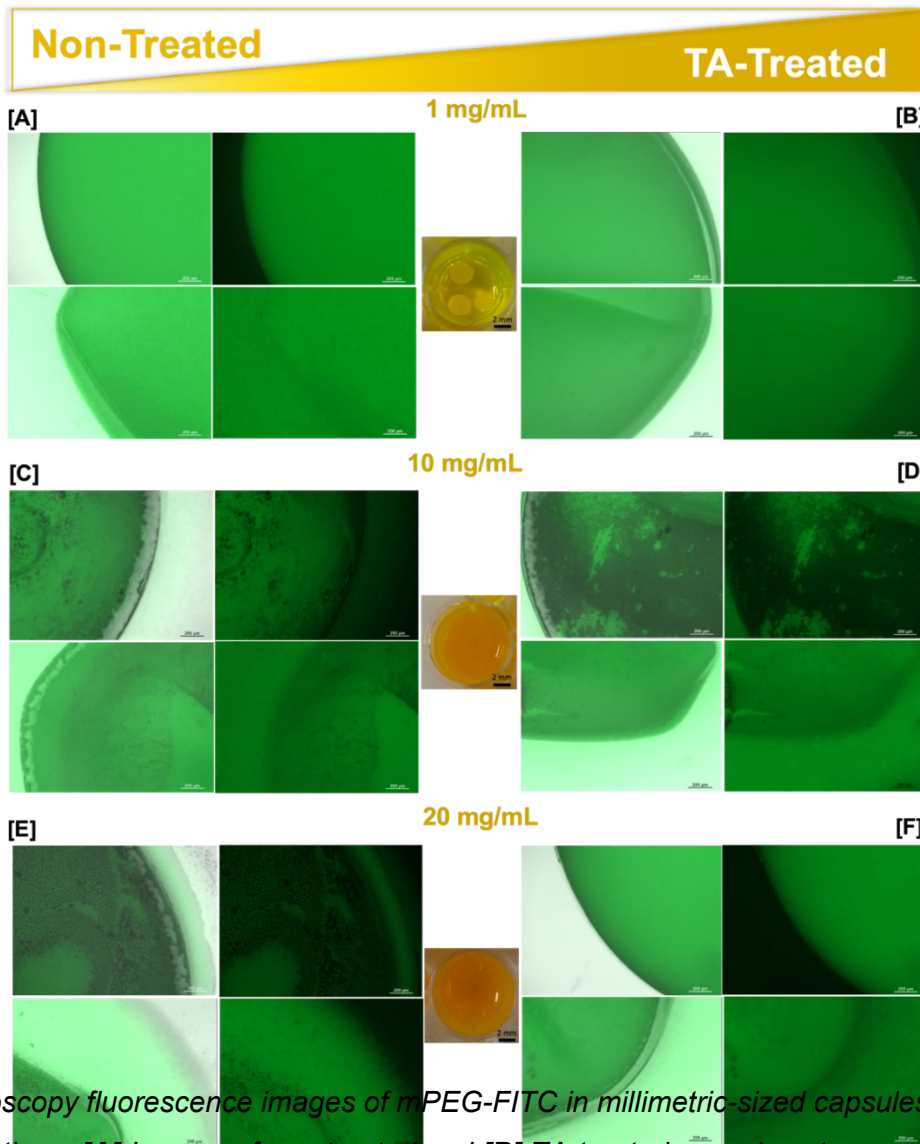


Fig. S9. Microscopy fluorescence images of mPEG-FITC in millimetric-sized capsules at different dye concentrations. **[A]** Images of non-treated and **[B]** TA-treated capsules at a concentration of 1.0 mg/mL of mPEG-FITC. **[C]** Images of non-treated and **[D]** TA-treated capsules at a concentration of 10 mg/mL of mPEG-FITC. **[E]** Images of non-treated and **[F]** TA-treated capsules at a concentration of 20 mg/mL of mPEG-FITC.

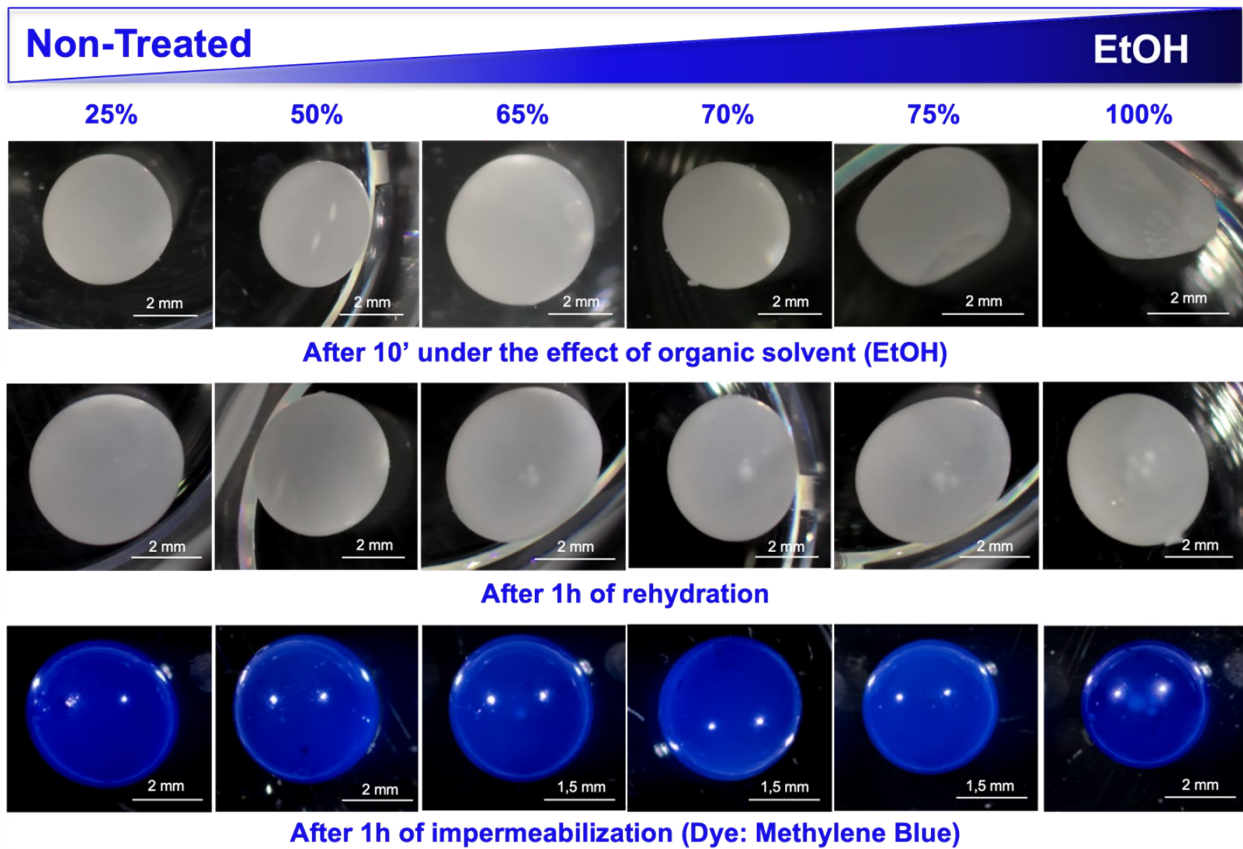
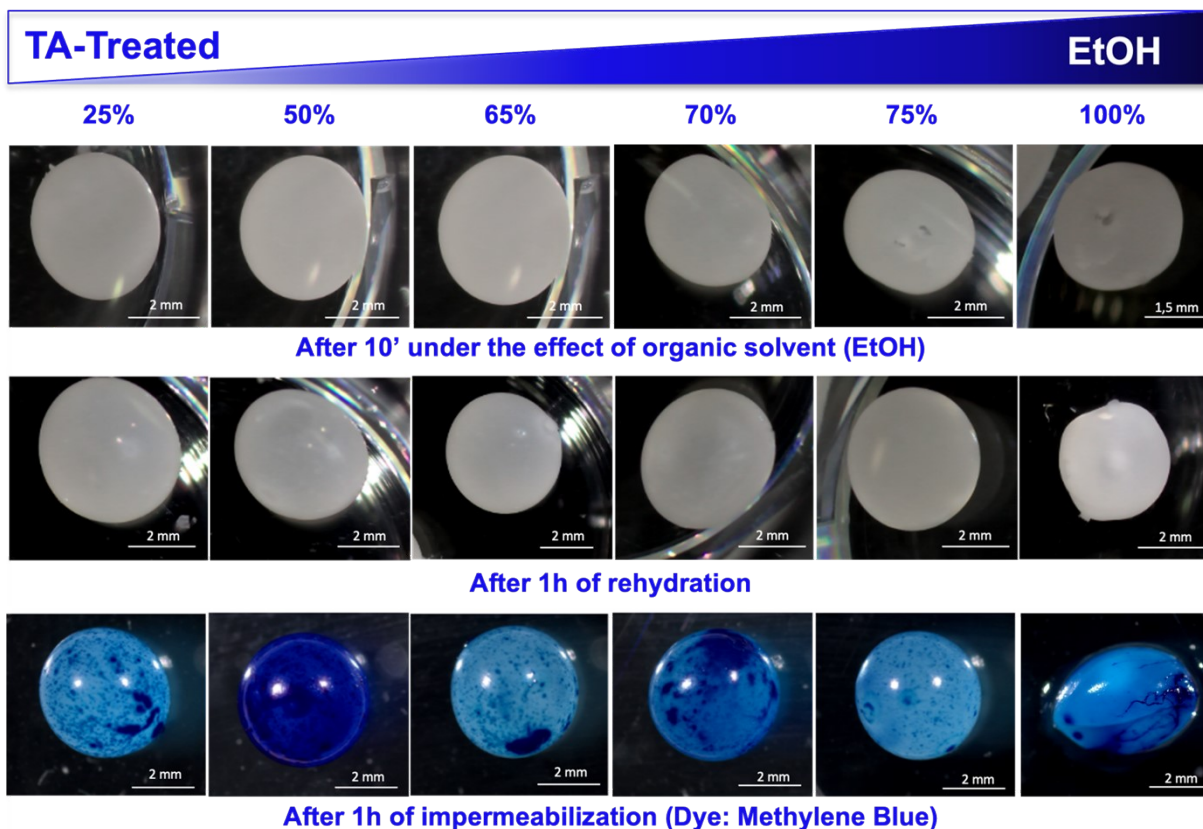


Fig. S10. Pictures of non-treated capsules exposed, for 10 minutes, to solutions of PBS with different relative volumes of ethanol (100% corresponding to a full ethanol solution); 1 hours after rehydration in distilled water; and after 1 hour exposure to MB.



Fi

g. S11. Pictures of TA-treated capsules exposed, for 10 minutes, to solutions of PBS with different relative volumes of ethanol (100% corresponding to a full ethanol solution); 1 hours after rehydration in distilled water; and after 1 hour exposure to MB.

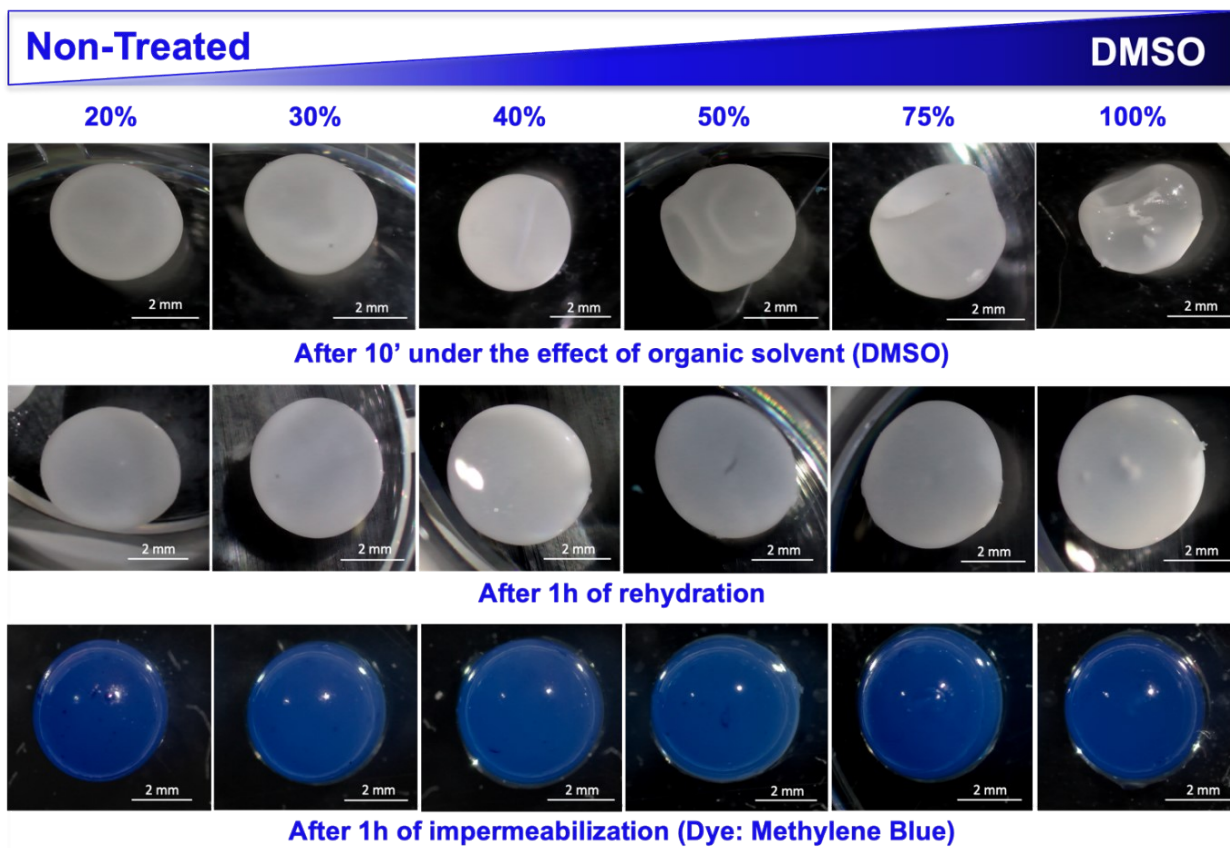


Fig. S12. Pictures of non-treated capsules exposed, for 10 minutes, to solutions of PBS with different relative volumes of DMSO (100% corresponding to a full DMSO solution); 1 hours after rehydration in distilled water; and after 1 hour exposure to MB.

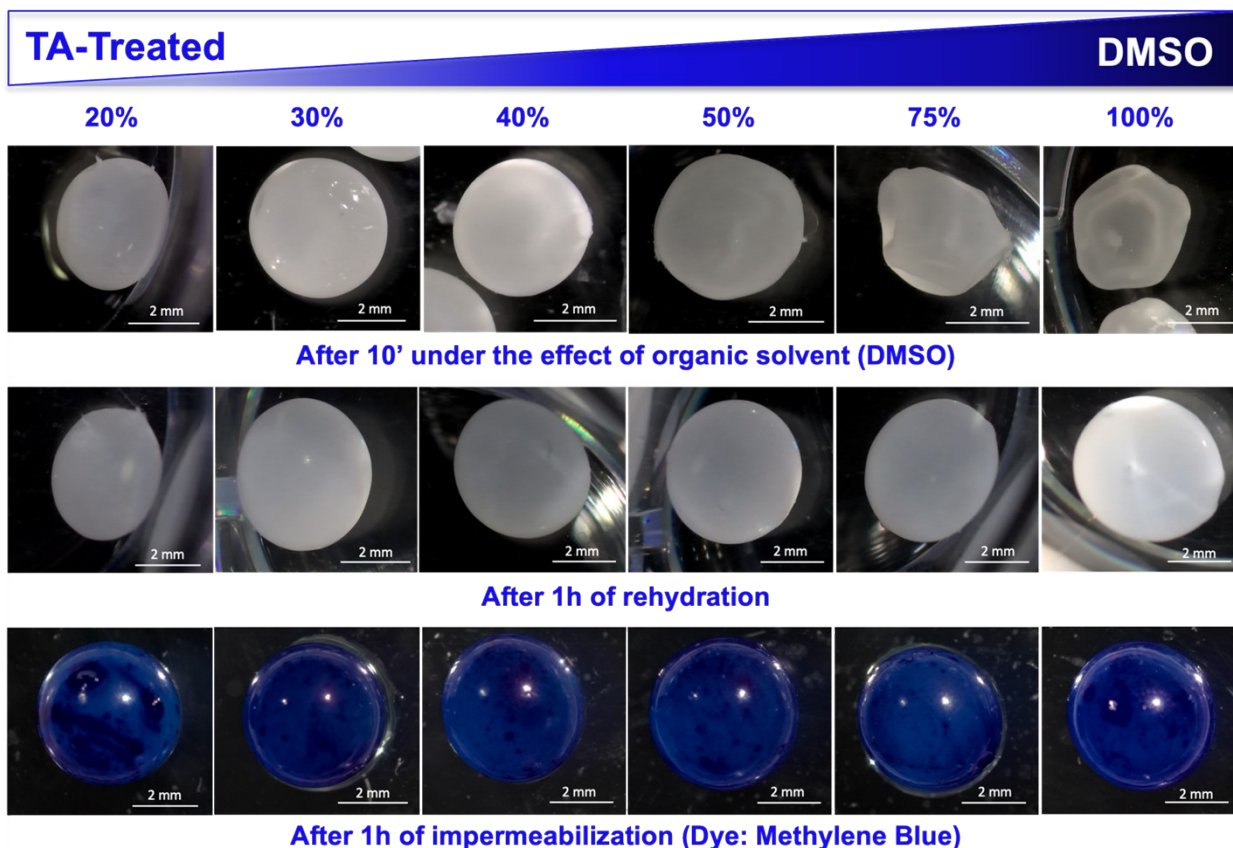


Fig. S13. Pictures of TA-treated capsules exposed, for 10 minutes, to solutions of PBS with different relative volumes of DMSO (100% corresponding to a full DMSO solution); 1 hours after rehydration in distilled water; and after 1 hour exposure to MB.

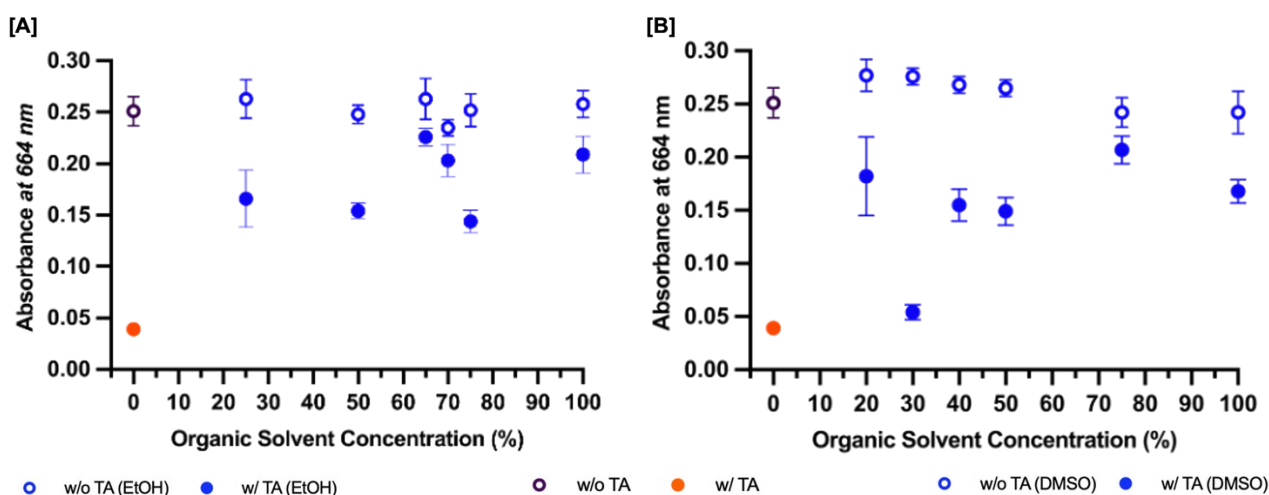


Fig. S14. Quantification of the absorbance, at 664 nm, detected in the inside of the capsules immersed in MB solution for 1 hour, after 10 min submission at different concentrations of **[A]** EtOH and **[B]** DMSO.

Table S2. Summary of kinetic analysis for all release profiles presented in this study, encompassing four different molecules (AR, MB, FG and mPEG-FITC), two different sized ranges (millimetric and micrometric,) for non-treated and TA-treated capsules at two different pH conditions (AcB pH 4 and PBS pH 7.4). The table reports the best-fitting model for each condition, corresponding kinetic constants, and statistical metrics including R^2 (Regression Coefficient); SSR (Sum of Square Residuals); RMSE (Root Mean Square Error) and AIC (Akaike's Information Criterion).

Condition	Best Fitting Curve Model	Kinetic Constants	Metrics			
			R^2	SSR	RMSE	AIC
AR_Ctr_PBS	Weibull	a = 15.7883 b = 124.5244 c = 0.4031	0.8553	11.3408	1.2728	9.3775
AR_TA_PBS	Weibull	a = 12.0115 b = 365.1989 c = 1.4122	0.9762	2.6244	0.6123	-0.8673
AR_Ctr_AcB	Weibull	a = 9.9836 b = 38.774 c = 0.9899	0.9354	3.0713	0.6624	0.2334
AR_TA_AcB	Weibull	a = 11.3483 b = 51.5223 c = 2.2134	0.9568	6.1484	0.9372	5.092
MB_Ctr_PBS	First Order	k = 0.0542	0.9693	13.6582	1.3968	8.679
MB_TA_PBS	--	--	--	--	--	--
MB_Ctr_AcB	Weibull	a = 45.9473 b = 218.7397 c = 1.1973	0.9842	31.3373	2.1158	16.4923
MB_TA_AcB	Weibull	a = 44.5185 b = 369.2511 c = 1.5814	0.9073	214.6784	5.5379	29.9626
FG_Ctr_PBS_RouteA	Weibull	a = 1330.7313 b = 12.2382 c = 0.2976	0.9588	6462.4079	30.3842	53.7949
FG_TA_PBS_RouteA	Weibull	a = 1095.5774 b = 163.7048 c = 0.6417	0.9593	23896.0864	58.4271	62.9489
FG_Ctr_AcB_RouteA	Weibull	a = 896.7979 b = 26.3885 c = 0.3361	0.9896	1116.1556	12.6274	41.5021
FG_TA_AcB_RouteA	Zero Order	k = 0.1197	0.9094	2208.595	17.7627	44.2794
FG_Ctr_PBS_RouteB	Weibull	a = 1368.3495 b = 27.0521 c = 0.7133	0.9637	1744.8352	49.9283	60.7482
FG_TA_PBS_RouteB	Weibull	a = 697.4802 b = 46.1129	0.9703	1857.7818	16.291	45.0686

		c = 0.2816				
FG_Ctr_AcB_RouteB	Weibull	a = 712.9966 b = 137.6773 c = 0.4902	0.9908	1656.5367	15.3834	44.266
FG_TA_AcB_RouteB	Weibull	a = 471.7737 b = 82.0673 c = 0.3157	0.9865	495.887	8.4167	35.8231
mPEG-FITC_Ctr	Weibull	a = 5.7489 b = 42.2389 c = 0.6896	0.9574	0.5023	0.2679	-12.441
mPEG-FITC_TA	Weibull	a = 4.8255 b = 535.6327 c = 0.69336	0.9993	0.0072	0.0322	-42.122
mPEG-FITC_Ctr_Liquid Core	Weibull	a = 250.9025 b = 37.6699 c = -3.302	0.9806	1295.902	13.6062	42.5474
mPEG-FITC_TA_Liquid Core	Weibull	a = 283.3526 b = 79.0149 c = -0.9395	0.9568	2935.4978	20.4782	48.2711
AR_Ctr_1 mg/mL	Weibull	a = 366.2912 b = 45.6208 c = 0.9767	0.9945	522.1311	5.7125	61.7653
AR_TA_1 mg/mL	Weibull	a = 391.7074 b = 145.7285 c = 1.2467	0.9943	1329.9667	9.1172	76.7251
AR_Ctr_2 mg/mL	Weibull	a = 775.0225 b = 75.0246 c = 1.0133	0.9940	4434.126	14.8898	114.027
AR_TA_2 mg/mL	Weibull	a = 631.9381 b = 102.673 c = 0.8999	0.9961	2065.1008	10.1614	98.744
AR_Ctr_Miniaturized Capsules	Weibull	a = 60.0564 b = 143.7274 c = 0.7728	0.9941	20.8617	1.1078	9.4799
AR_TA_Miniaturized Capsules	Weibull	a = 36.1619 b = 362.7847 c = 0.7475	0.9900	11.1339	0.08093	-1.1947